Chemical Engineering Journal 157 (2010) 466–474

Contents lists available at ScienceDirect

Chemical Engineering Journal

journal homepage: www.elsevier.com/locate/cej

Adsorption of phenols by magnetic polysulfone microcapsules containing tributyl phosphate

Juanjuan Yin, Rui Chen, Yongsheng Ji, Chuande Zhao, Guanghui Zhao, Haixia Zhang*

State Key Laboratory of Applied Organic Chemistry, Lanzhou University, Lanzhou 730000, China

ARTICLE INFO

Article history:
Received 30 June 2009
Received in revised form 4 December 2009
Accepted 7 December 2009

Keywords:
Adsorption
Phenols
Polysulfone
Tributyl phosphate
Magnetic

ABSTRACT

Porous polysulfone (PSF) microcapsules containing both tributyl phosphate (TBP) as extractant and magnetic nanoparticles (Fe_3O_4) that help the isolation operation have been successfully prepared for the first time using a phase inversion method. Several techniques, including Fourier transform infrared (FT-IR), scanning electron microscope (SEM), vibrating sample magnetometer (VSM) and thermogravimetric analysis (TGA) have been used to characterize the microcapsules. The adsorption of four kinds of phenols (4-chlorophenol, 4-CP; 2-chlorophenol, 2-CP; 4-nitrophenol, 4-NP; phenol, Ph) from aqueous solutions on to the magnetic microcapsules has then been studied in a batch system as a function of contact time (5–60 min), initial phenols concentrations (about 99–1050 mg/L) and pH (2–12). The results show that increasing the initial concentration of the phenols and the adsorption time favored the adsorption. In contrast, the adsorption decreased for pH > 6. Adsorption data were modeled using Freundlich and Langmuir adsorption isotherms and the appropriate parameters were calculated. The Freundlich equation provided a better fit for the four phenols than the Langmuir equation. Simultaneously, various kinetic models including pseudo-first-order, pseudo-second-order and intraparticle diffusion were investigated to determine the mechanism of adsorption. The experimental data fitted the pseudo-second-order kinetic model well, and showed that intraparticle solute diffusion was not the only rate-controlling sorption step. In an investigation of potential industrial applications, it is demonstrated that the final concentration of phenols treated with the novel magnetic microcapsules will be within allowed limits. After six extraction and regeneration cycles, the microcapsules were unchanged and showed almost the same adsorption ability. These results demonstrate that these novel magnetic microcapsules have potential applications in the treatment of environmental pollution caused by phenols. This study broadens the application of microcapsules, which are, at the moment, mainly used to remove heavy metals from water.

1. Introduction

Phenol and its derivatives are versatile raw materials in chemical industry [1], and widely used in many industrial activities such as the petrochemical industries, kraft pulp mills, olive oil production, and various other chemical manufacturing industries. As a result, phenols are extensively present in the effluents of these manufacturing plants and are inevitably introduced into waste water. Most of them are toxic [2], and have a low permissible safety levels. For instance, the permitted concentration of volatile phenols is 0.5 mg/L for standard A effluent and 2.0 mg/L for standard C effluent, according to the Chinese Integrated Water Discharge Standard (GB 8978-1996). Therefore, it is considered necessary to remove phenols from effluents before discharging them into the water stream.

In order to remove phenolic compounds from aqueous solution, various treatment technologies with their inherent limitations and merits are available. These include oxidation [3,4], ion exchange [5,6], adsorption [7,8] and solvent extraction [9,10]. Adsorption technology is currently being applied extensively to the removal of organic and inorganic micro-pollutants from aqueous solutions. Several adsorbents have been investigated by previous researchers such as activated carbon [11,12], natural materials [13–17] and synthetic resins [5,18]. The advantages associated with these solid-phase adsorbents are easy isolation, high adsorption capacity and an effective regeneration process [19]. However, some deficiencies such as intraparticle resistance and low rates of absorption are present. In contrast, liquid–liquid extraction, which is an effective extraction method, demonstrates a rapid rate of absorption [20]. However, the organic solvents used in this procedure are usually volatile, toxic, flammable and easily form an emulsion which causes loss of extractant and damage to water supplies [20,21].

To overcome the disadvantages of both solid-phase extraction and liquid-phase extraction, and at the same time make best

* Corresponding author. Tel.: +86 931 4165997; fax: +86 931 8912582.
E-mail address: zhanghx@lzu.edu.cn (H. Zhang).

1385-8947/$ – see front matter © 2009 Published by Elsevier B.V.
doi:10.1016/j.cej.2009.12.008

use of their advantages, the organic extractant can be encapsulated with a polymer membrane. In the solvent microcapsule, liquid-phase extractant fills the supporting porous structure and the core of microcapsules [21]. This can allow phenols to diffuse rapidly into the microcapsules from the surface porous structure. Compared to conventional solid-phase adsorbents, solvent microcapsules are characterized by rapid adsorption. Furthermore, compared to conventional liquid–liquid extraction, solvent microcapsules have several advantages, such as minimal use of organic solvents and ease of phase separation [22]. Until now, most applications of microcapsules have focused on the removal of heavy metals, such as Co^{2+} [23], Ni^{2+} [24] and Cr^{6+} [25].

To our knowledge, the encapsulation of TBP (a specific extractant for phenols [26]) within PSF microcapsules has never been investigated. This forms the subject of this report. However, microcapsules with small diameters [22–25] are very difficult to separate from water after the adsorption. Magnetic separation is considered to be a promising method to achieve rapid separation and it has the capability to treat a large amount of wastewater very rapidly [23]. Therefore, in the present work, the magnetic microcapsules have been prepared by wrapping TBP and Fe_3O_4 with PSF. The magnetic microcapsules were then introduced into a solution containing the targeted phenols. The effects of contact time, initial concentration of phenols and pH on the phenols adsorption have been investigated. A potential industrial application of the microcapsules is also reported.

2. Materials and methods

2.1. Materials and instruments

Polysulfone (PSF), with an intrinsic viscosity of 0.56, was purchased from Dalian Polysulfone plastic Co. Ltd. (Dalian, China). Ferrous chloride ($FeCl_2{\cdot}4H_2O$) and ferric chloride ($FeCl_3{\cdot}6H_2O$) were obtained from Tianjin Chemicals Corporation (Tianjin, China). N,N-dimethylformamide (DMF) and ethanol were purchased from Tianjin Guangfu Chemical Reagent Co. Ltd. (Tianjin, China). Phenol (99.5%, assay) was purchased from Tianjin Guangfu Fine Chemical Research Institute (Tianjin, China). 2-chlorophenol (2-CP), 4-chlorophenol (4-CP), 4-nitrophenol (4-NP) and sodium dodecyl sulfate (SDS) were obtained from Shanghai Chemical Reagent Co. (Shanghai, China). Tributyl phosphate (TBP) was purchased from Beijing Chemical Reagent Co. (Beijing, China). All reagents were of analytical purity grades and used without any further purification.

The adsorption experiments were carried out at constant temperatures controlled by a SHA-C Shaker (Jiangsu, China) with a precision of ±0.5 K. The absorbency was recorded by a TU-1810 spectrophotometer from Purkinje Co. (Beijing, China). The optimum UV wavelength for each compound was: 4-CP at 281 nm, 2-CP at 273 nm, 4-NP at 317 nm and Ph at 270 nm.

2.2. Preparation of magnetic particles

Magnetic microspheres were prepared via the co-precipitation method [27]. Briefly, a 25 mL mixed solution of 0.8 M iron(III) chloride and 0.4 M iron(II) chloride was prepared using water with 3 vol.% HCl. The mixture was next added to 250 mL of ammonia solution (5.23 vol.%) with magnetic stirring at 1100 rpm. The reaction was allowed to proceed for 1 h. The Fe_3O_4 nanoparticles were collected by a magnet and thoroughly washed with distilled water to remove excess amounts of ammonium hydroxide, then washed several times with methanol. The Fe_3O_4 magnetic nanoparticles were dried under vacuum at room temperature.

2.3. Preparation of TBP/Fe_3O_4@PSF microcapsules

Preparation of the dispersed phase. TBP/Fe_3O_4@PSF microcapsules were prepared by the phase inversion precipitation technique [28]. The experimental methodology for synthesis of microcapsules is based on the following outline: 1.2 g PSF was dissolved in 16 mL DMF to obtain the PSF solution, then 0.8 mL TBP and 0.1 g Fe_3O_4 magnetic nanoparticles (which were dispersed into 4 mL DMF by ultrasonication) were added into the PSF solution and stirred for 2 h at room temperature. In this way a dispersed phase containing TBP, Fe_3O_4 magnetic nanoparticles and PSF was obtained.

Preparation of continuous phase. This was achieved by mixing the SDS solution (0.5 wt.% sodium dodecylbenzenesulfonate in aqueous solution) with ethanol in 1:1 volume ratio

Preparation of TBP/Fe_3O_4@PSF microcapsules. The dispersed phase was injected into the continuous phase using a 0.45 mm diameter syringe needle. The magnetic microcapsules obtained were separated from the resulting solution by a magnet, rinsed with deionized water several times, and kept in deionized water overnight to remove DMF completely. Finally, the microcapsules were air-dried at room temperature.

2.4. Characterization

The products obtained were characterized using scanning electron microscopy (SEM, JSM-5600LV, JEOL, Japan; and JSM-6701F, JEOL, Japan) and Fourier transform infrared spectrometer (FT-IR, Nicolet Nexus 670, USA). Magnetic properties were measured using a vibrating sample magnetometer (VSM, Lakeshore7304, USA). The encapsulation capacity of the TBP was measured by a thermogravimetric analyzer (TGA, STA449, Netzsch, Germany).

2.5. Adsorption and regeneration experiments

The adsorption experiment was carried out in a batch reactor, held in a water bath. Twenty-five milligrams of TBP/Fe_3O_4@PSF microcapsules were added into 25 mL flasks containing 10 mL of 4-CP, 2-CP, 4-NP or Ph solution. The flasks were sealed and shaken in the shaker. After the adsorption, the magnetic microcapsules were isolated by an external magnetic field and the concentrations of phenols in the supernatants determined by UV–vis spectrophotometer at the appropriate optimum UV wavelengths. The amount of 4-CP, 2-CP, 4-NP and Ph adsorbed was calculated by the difference between the initial and final concentrations. The effects of pH (2–12), contact time (5–60 min) and initial phenols concentrations (100–1000 mg/L) were studied. The variation of the uptake of 4-CP, 2-CP, 4-NP and Ph with adsorption time was investigated using kinetic models.

Regeneration experiments for the TBP/Fe_3O_4@PSF microcapsules were conducted as followings: (i) 250 mg of TBP/Fe_3O_4@PSF microcapsules were put into 10 mL of mixture containing 4-CP (4.43 mg/L), 2-CP (4.66 mg/L), 4-NP (4.46 mg/L) and Ph (5.02 mg/L) at room temperature (about 20 °C) for 1 h to adsorb phenols. (ii) After extraction, the microcapsules were isolated from the phenols solutions using an external magnetic field, were soaked twice in 1 mL NaOH solution (1.0 M) for 30 min at room temperature, and then the eluate collected to determine the concentrations of phenols using high-performance liquid chromatography (HPLC) at a wavelength of 280 nm. (iii) The microcapsules were washed with deionized water until neutral and then used for another cycle. The procedure was repeated six times to study the stability of the TBP/Fe_3O_4@PSF microcapsules.

The chromatographic system consisted of a Waters 600 high-performance liquid chromatographic pump, and a Waters 600 chromatographic work station. An analytical reversed-phase C18 column (5 μm, 4.6 mm × 250 mm, Dima Technology) was used. The

Fig. 1. Photo of TBP/Fe_3O_4@PSF microcapsules.

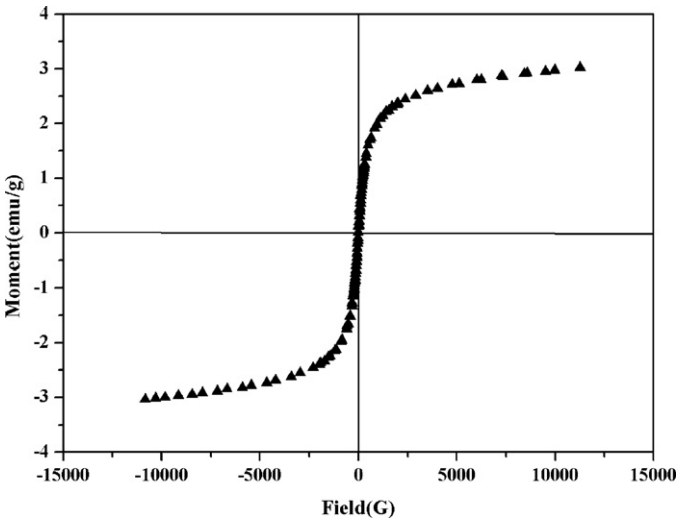

Fig. 3. VSM magnetization curve of TBP/Fe_3O_4@PSF microcapsules.

mobile phase consisted of Milli-Q water containing 1% (v/v) acetic acid and 0.5 g L^{-1} of KCl as solvent A, and acetonitrile as solvent B. The flow-rate of the mobile phase was 1 mL min^{-1}. The gradient profile was 25% B at 0 min, 50% B at 25 min, 100% B at 30 min, and held constant for 10 min. The target compounds were identified by the relative retention time and diode array detection (model 2996, Waters, Milford, MA, USA).

3. Results and discussion

3.1. Characterization of TBP/Fe_3O_4@PSF microcapsules

3.1.1. Morphological observation

Fig. 1 shows a photo of the microcapsules, illustrating that the microcapsules have good, regular shapes. Typical SEM photographs were taken of the microcapsules prepared as a dispersed phase containing 1.2 g PSF, 0.8 mL TBP and 0.1 g Fe_3O_4 in 20 mL DMF and a continuous phase containing 50 mL 0.5 wt.% SDS solution and ethanol (1:1 volume ratios) and are shown in Fig. 2. Fig. 2(a) illustrates the general view of the microcapsule which is not completely spherical, but is similar to that of a hamburger. Fig. 2(b) shows the outer surface of the microcapsule. Micro-pores can also be clearly observed on the surface of the microcapsules, which help to reduce mass transfer resistance owing to the liquid-phase extractant filling the supported micro-pores [21]. The liquid-phase extractant made phenols rapidly diffuse into the microcapsules from the surface micro-pores. Furthermore, the liquid-phase in the core of microcapsule can adsorb much more rapidly than conventional solid adsorbents. These micro-pores allow phenols to access, but TBP was not released into aqueous solution because of its hydrophobic character.

3.1.2. Vibrating sample magnetometer characterization

In the preparation of the microcapsules for potential magnetic separation, it is of utmost importance that the microcapsules should possess sufficiently strong magnetic properties, which can be characterized with a VSM. The magnetization curve from the VSM data is shown in Fig. 3. The curve has a typical shape, being symmetrical about the origin. This feature is characteristic of superparamagnetism, illustrating that the microcapsules respond magnetically to an external magnetic field and this response vanishes upon the removal of the field (at the origin). The key parameter to note is the saturation magnetization (S), which is a measure of the maximum magnetic strength of the materials. The S value of the microcapsules (3.2 emu/g) indicates that the microcapsules possess sufficient magnetic strength [29]. Fig. 4 displays a

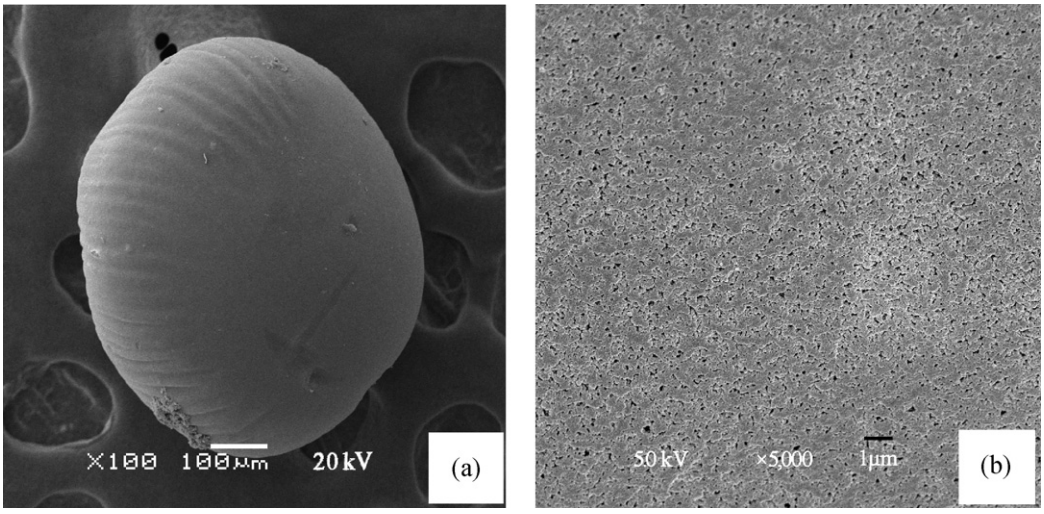

Fig. 2. SEM image of TBP/Fe_3O_4@PSF microcapsules: (a) general view; (b) outer surface.

Fig. 4. Photograph of TBP/Fe_3O_4@PSF microcapsules attracted by a conventional magnet.

picture in which the magnetic microcapsules were being attracted by a conventional magnet.

3.1.3. FT-IR

To ascertain the presence of TBP in the microcapsules, the infrared spectrum of the microcapsules was obtained and is shown in Fig. 5. The FT-IR spectra of Fe_3O_4@PSF microcapsules (curve (a)) gave characteristic bands for PSF at 3095.68 cm^{-1} (C–H stretching of aromatic ring), 1322.54 cm^{-1} and 1103.64 cm^{-1} (asymmetrical and symmetrical stretching vibration of O=S=O), 1247.58 cm^{-1} (stretching vibration of aromatic ether bond). In the same way, the features (curve (b)) around 1278.71 cm^{-1} (stretching vibration of P=O) and 1028.27 cm^{-1} (antisymmetric stretching vibration of P–O–C) are characteristic peaks of TBP. All these features can be found in curve (c) clearly showing that TBP has been successfully encapsulated in the microcapsules.

3.1.4. Thermogravimetric analysis

TGA was employed to quantify the amount of TBP encapsulated in the microcapsules. The analysis was carried out in nitrogen gas to prevent the oxidation of the microcapsules. The TGA graph is shown in Fig. 6. The temperature was increased from room temperature to 800 °C at a rate of 10 °C/min. The microcapsules lost weight

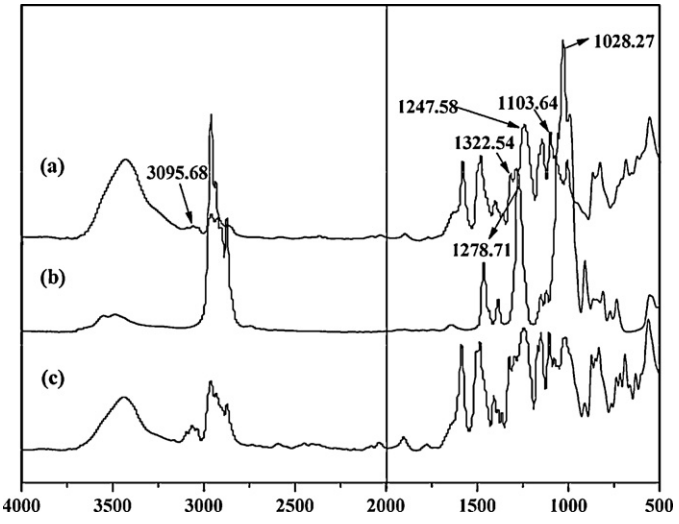

Fig. 5. Infrared spectrum of the microcapsules. (a) Fe_3O_4@PSF microcapsules; (b) TBP; (c) TBP/Fe_3O_4@PSF microcapsules.

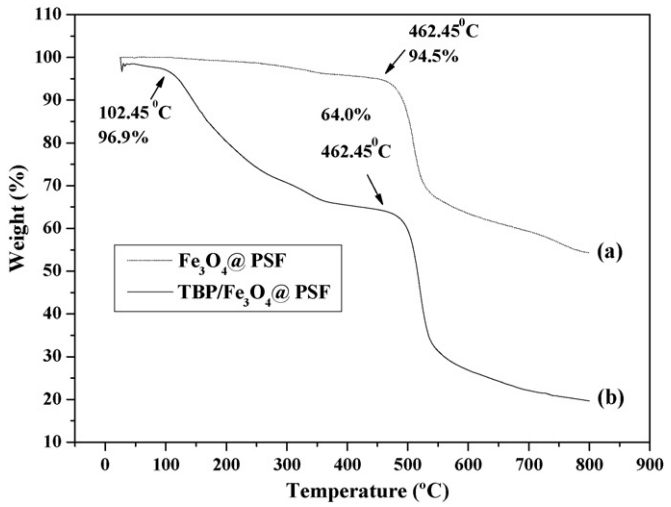

Fig. 6. TGA of the microcapsules. (a) Fe_3O_4@PSF microcapsules; (b) TBP/Fe_3O_4@PSF microcapsules.

over three regions of temperature. The weight loss between room temperature and 102.45 °C was attributed to the water adsorbed in the microcapsules. In the range 102.45 °C to about 462.45 °C, the weight loss was due to the decomposition of TBP, while PSF began to decompose at 462.45 °C. The encapsulation capacity of the microcapsules as calculated was 32.9%, which was slightly better than that reported elsewhere [30,31]. The encapsulation efficiency was considered to be very satisfactory. The TGA results also showed that the microcapsules could be used below 100 °C.

3.2. Adsorption studies

3.2.1. Effect of contact time and initial concentration

Fig. 7(a, 4-CP; b, 2-CP; c, 4-NP; d, Ph) depicts the effect of contact time on the adsorption of phenols at various initial concentrations (a, 4-CP 99.4–1070 mg/L; b, 2-CP 314.8–1050.3 mg/L; c, 4-NP 305.9–992.5 mg/L; d, Ph 403–1030.2 mg/L). It was found that the rate of uptake of phenols was rapid in the first 5 min and approximately 90% of adsorption was completed within 15 min for 4-CP, 2-CP, 4-NP and Ph. The amount of adsorption increased with increasing contact time and equilibrium was achieved within 30 min.

It was also found that increasing the initial phenols concentration resulted in increased phenols uptake and the quantity of the four phenols absorbed with the same conditions was in the order: 4-CP > 2-CP > 4-NP > Ph. This different degree of adsorption may be explained in terms of the hydrophobic character of the four phenols. The n-octanol/water partition coefficient is an important hydrophobic parameter. This is the ratio of the chemical's concentration in n-octanol to that in water in a two-phase system at equilibrium. Since the measured values of the partition coefficient range from less than 10^{-4} to greater than 10^8 (at least 12 orders of magnitude), the logarithm, log P (known as the hydrophobic parameters), is commonly used to describe a compound's lipophilic or hydrophobic properties [32]. As shown in Fig. 8, the quantity of phenol adsorbed increased with the increase of log P values obtained from United States National Library of Medicine. That is, hydrophobic interaction may be one of the driving forces.

3.2.2. Effect of solution pH

The effect of solution pH on the adsorption of phenols by the microcapsules was examined and the results are presented in Fig. 9. It was found that an alkaline solution, with pH higher than 8.0, was not favorable for the adsorption. This phenomenon could be

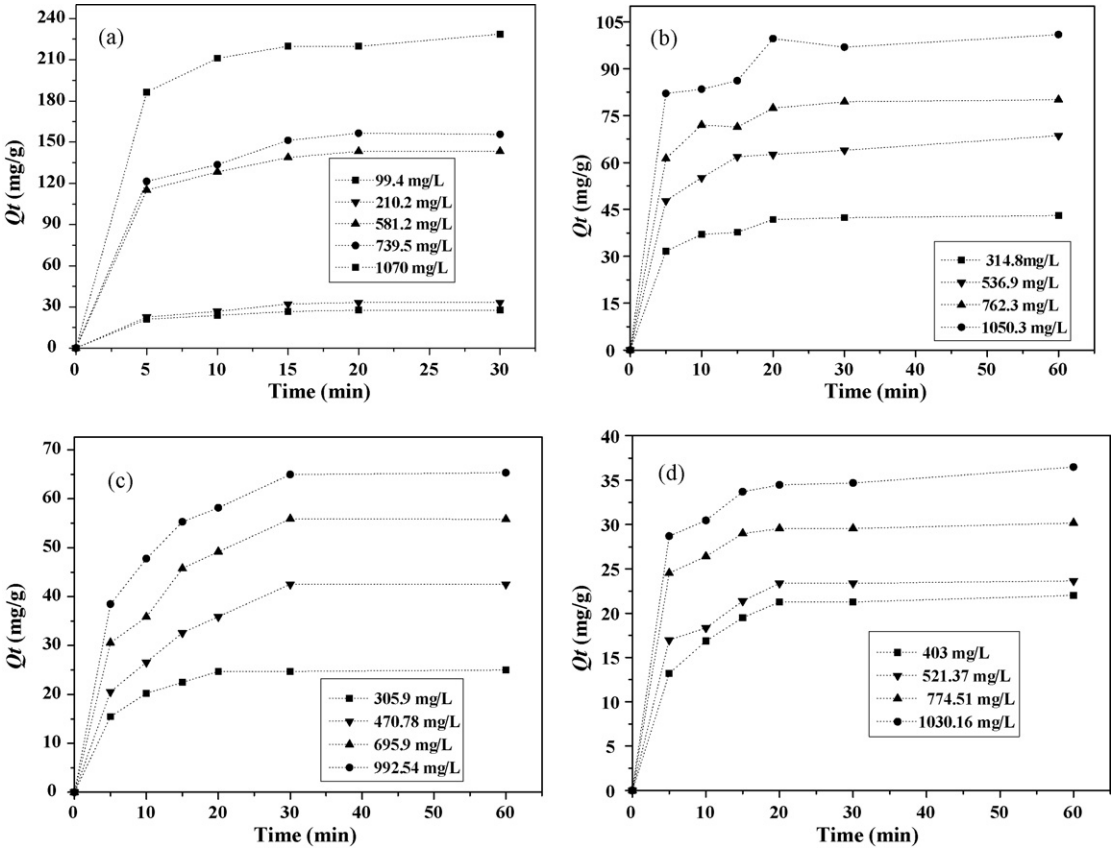

Fig. 7. Effect of contact time and initial phenols concentration on phenols uptake from aqueous solutions (20 °C, pH 6): (a) 4-CP; (b) 2-CP; (c) 4-NP; (d) Ph.

explained in three ways. Firstly, phenols are in a negative ionic form in alkaline solution, which does not favor adsorption. Secondly, the intermolecular hydrogen bond (OH···O=P) between the phenolic hydroxyl group and the phosphoryl group on TBP at pH < pKa, is favorable for adsorption. Phenols are weak acid compounds with pKa ≈ 9.41 (4-CP), 8.56 (2-CP), 7.15 (4-NP), 9.99 (Ph) and would be dissociated at pH > pKa, which leads to a disappearance of hydrogen bonding. Thirdly, phenolic acids have lower solubility at low pH in water.

3.3. Adsorption modeling

3.3.1. Sorption kinetics of phenols

3.3.1.1. The pseudo-first-order kinetic model. To investigate the mechanism of adsorption, a simple kinetic model was used to test the experimental data, by applying the Lagergren equation [33], which is the first equation describing the adsorption of liquid–solid systems based on solid capacity.

$$\ln(Q_e - Q_t) = \ln\ Q_e - k_1 t \quad (1)$$

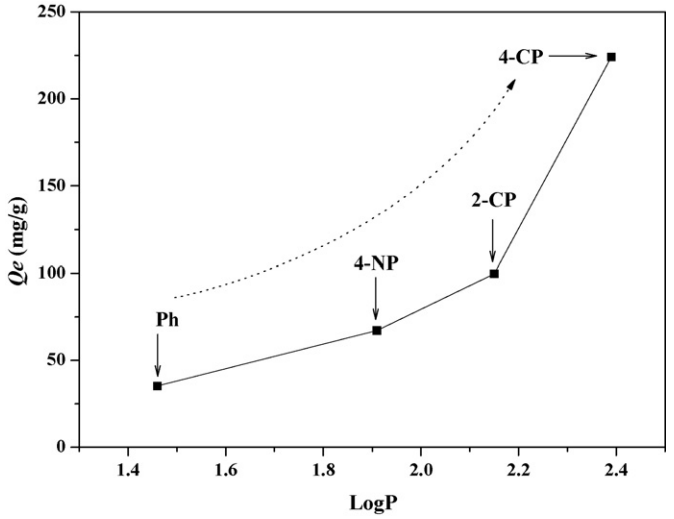

Fig. 8. The correlation of log *P* and Q_e of phenols (initial phenols concentration = 1040 mg/L; contact time = 1 h, 20 °C, pH 6.0).

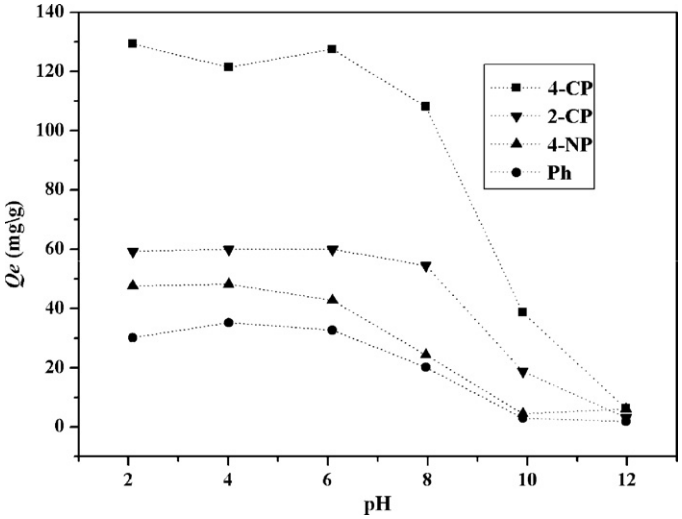

Fig. 9. Effect of initial pH on the phenols uptake from aqueous solutions (initial phenols concentration = 550 mg/L; contact time = 1 h, 20 °C).

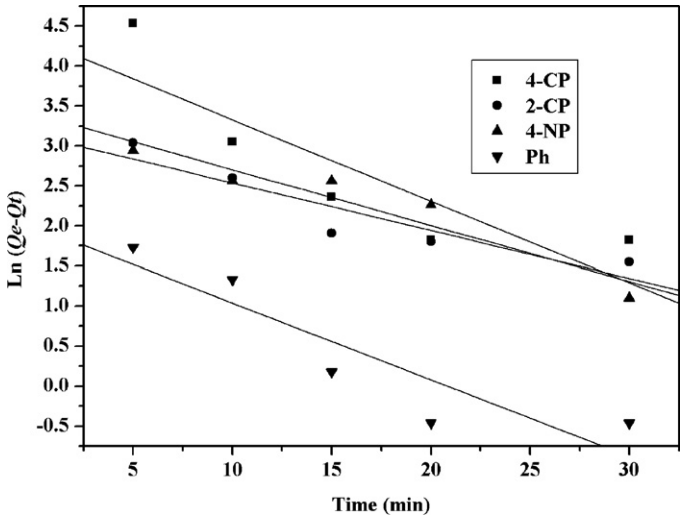

Fig. 10. The fitting of pseudo-first-order model for different phenols on TBP/Fe_3O_4@PSF microcapsules (initial phenols concentration = 500 mg/L; pH 6.0, 20 °C).

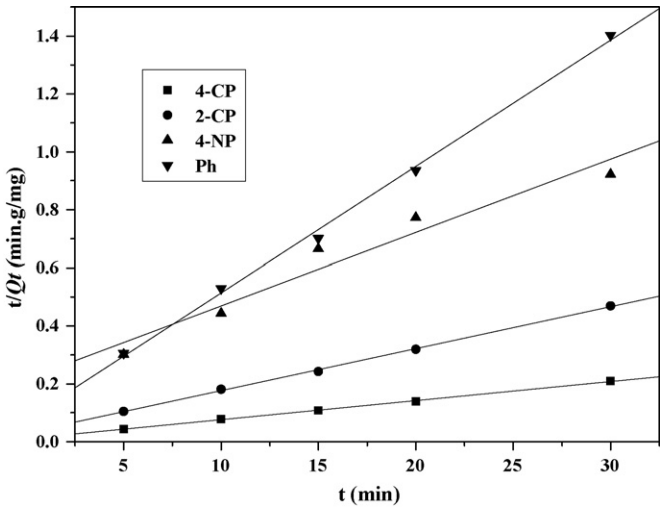

Fig. 11. The fitting of pseudo-second-order model for different phenols on TBP/Fe_3O_4@PSF microcapsules (initial phenols concentration = 500 mg/L; pH 6.0, 20 °C).

where Q_t is the quantity of phenols (mg/g) adsorbed on the TBP/Fe_3O_4@PSF microcapsules after various times t, Q_e is the maximum adsorption capacity (mg/g) and k_1 is the pseudo-first-order rate constant for the adsorption process (min^{-1}). The values of $\ln(Q_e - Q_t)$ were calculated from the kinetic data. In order to confirm the applicability of the model, a plot of $\ln(Q_e - Q_t)$ against t should be a straight line. In a real first-order process, the experimental $\ln(Q_e)$ should be equal to the intercept of the straight line. The slope and intercept of each linear region in Fig. 10 are used to calculate the first-order constant (k_1) and Q_e (see Table 1). It is clear that the R^2 values are relatively low and the experimental Q_e values did not agree with the calculated Q_e values from the linear plots. These results showed that the pseudo-first-order model did not satisfactorily predict the kinetics of phenols adsorption on to the TBP/Fe_3O_4@PSF microcapsules.

3.3.1.2. The pseudo-second-order kinetic model. The adsorption kinetics can also be described by a pseudo-second-order equation [34,35]:

$$\frac{t}{Q_t} = \frac{1}{k_2 Q_e^2} + \frac{t}{Q_e} \quad (2)$$

where Q_t is the amount of phenol (mg/g) adsorbed on the TBP/Fe_3O_4@PSF microcapsules after various times t, Q_e is the maximum adsorption capacity (mg/g) for the pseudo-second-order adsorption and k_2 is the pseudo-second-order rate constant for the adsorption (g/mg min).

Fig. 11 shows the curves obtained from the experimental data (t/Q_t) vs. t. The kinetic parameters were calculated and are listed in Table 1. Higher correlation coefficients for the pseudo-second-order model and calculated Q_e values being close to the experimental data indicate that the absorption of phenols on to TBP/Fe_3O_4@PSF microcapsules can be more favorably approximated by a pseudo-second-order model than the pseudo-first-order one.

3.3.1.3. The intraparticle diffusion model. The adsorbate transport from the solution phase to the surface of the adsorbent particles occurs in several steps. The overall adsorption process may be controlled by any one of several steps, e.g. film or external diffusion, pore diffusion, surface diffusion and adsorption on the pore surface, or a combination of several steps [36]. The possibility of intraparticle diffusion was explored by using the intraparticle diffusion model [37], which is expressed as:

$$Q_t = k_3 t^{1/2} + C \quad (3)$$

where k_3 is the intraparticle diffusion constant (mg/g $min^{1/2}$), and the value of the intercept C is a constant that gives a measure of the thickness of the boundary layer, i.e., the larger the value of C the greater is the boundary layer effect [38]. From the plots in Fig. 12, the values of k_3, C and R_3^2 were calculated and are given along with the correlation factors in Table 1. According to this model, plots of Q_t vs. $t^{1/2}$ should be linear and pass through the origin if intraparticle diffusion is the rate-controlling step [39]. On the other hand, if the plots are linear but do not pass through the origin the rate of adsorption may be controlled by intraparticle diffusion together with other kinetic effects. As can be seen from Fig. 12, the line did not pass through the origin. This indicated that particle diffusion was involved in the adsorption process but it was not the only rate-limiting step. Other mechanisms were involved.

Table 1
The rate constants of adsorption kinetic model for different phenols on TBP/Fe_3O_4@PSF microcapsules.

Compounds	Q_e[a] (mg/g)	Pseudo-first-order			Pseudo-second-order			Intraparticle diffusion		
		Q_e[b] (mg/g)	k_1 (min^{-1})	R_1^2	Q_e[b] (mg/g)	k_2 (g/mg min)	R_2^2	k_3 (mg/g $min^{1/2}$)	C	R_3^2
4-CP	149.44	39.54	0.0725	0.8367	151.5	0.0043	0.9994	7.5996	105.8	0.9196
2-CP	68.64	22.96	0.0596	0.8588	68.96	0.0067	0.999	4.2662	42.56	0.9221
4-NP	35.54	29.90	0.0698	0.9077	39.52	0.0030	0.9505	3.6738	10.52	0.9242
Ph	22.64	6.190	0.0657	0.6845	22.94	0.0245	0.9975	1.3655	14.85	0.8569

[a] Experimental.
[b] Calculated.

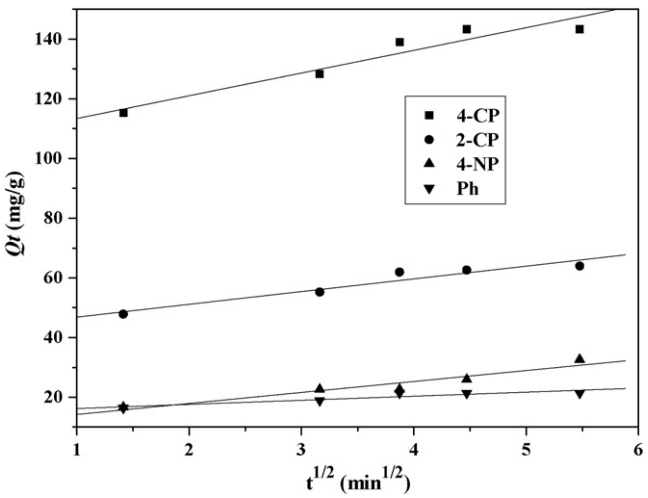

Fig. 12. The fitting of intraparticle diffusion model for different phenols on TBP/Fe_3O_4@PSF microcapsules (initial phenols concentration = 500 mg/L; pH 6.0, 20 °C).

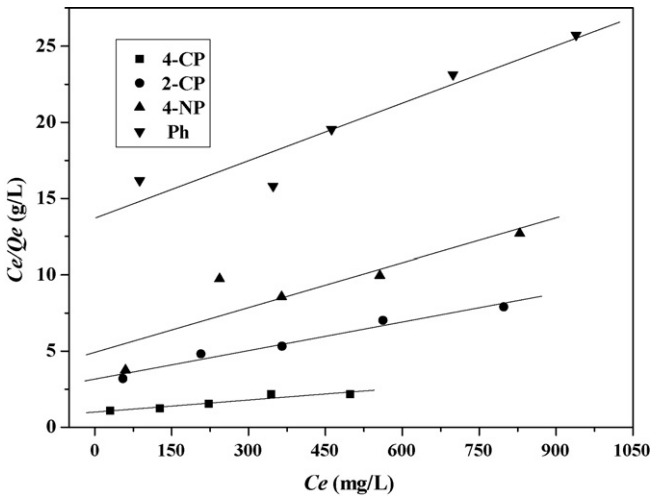

Fig. 13. Langmuir plot for different phenols adsorption onto TBP/Fe_3O_4@PSF microcapsules (contact time = 1 h; pH 6.0, 20 °C).

3.3.2. Sorption isotherm of phenols

The equilibrium isotherms are very important for understanding the adsorption systems. There are several isotherm equations available for analyzing experimental sorption equilibrium data. The most frequently used for phenols solutions are the Langmuir adsorption isotherm and Freundlich equations. The Langmuir adsorption isotherm assumes monolayer adsorption on to a surface containing a finite number of adsorption sites, with uniform strategies of adsorption and no transmigration of adsorbate in the plane of the surface [40]. In contrast to Langmuir, the Freundlich isotherm is based on the assumption that the adsorption occurs on heterogeneous sites with non-uniform distribution of energy levels. The Freundlich isotherm describes reversible adsorption and is not restricted to the formation of a monolayer [41].

The linear form of the Langmuir and Freundlich equations can be represented as follows:

$$\text{Langmuir equation}: \quad \frac{C_e}{Q_e} = \frac{1}{K_L Q_{\max}} + \frac{C_e}{Q_{\max}} \tag{4}$$

$$\text{Freundlich equation}: \quad \ln Q_e = \ln K_f + \frac{1}{n} \ln C_e \tag{5}$$

where C_e (mg/L) is the concentration of the phenol solution at equilibrium and Q_e (mg/g) is the amount of sorption at equilibrium. In the Langmuir equation, $Q_{\max}$ is the maximum sorption capacity and K_L is the Langmuir constant. These constants can be evaluated from the intercept and the slope, respectively, of the linear plot of experimental data of C_e/Q_e vs. C_e (Fig. 13). In the Freundlich equation, K_f and $1/n$ are empirical constants. These constants can also be evaluated from the intercept and slope of the linear plot of $\ln Q_e$ vs. $\ln C_e$ (Fig. 14). The values of the isotherm constants are presented in Table 2. It is observed that the equilibrium data fitted the Freundlich isotherm better than the Langmuir isotherm, from the relative R^2 values. It could be deduced that phenols are adsorbed on to heterogeneous sites with a non-uniform distribution of energy levels [41],

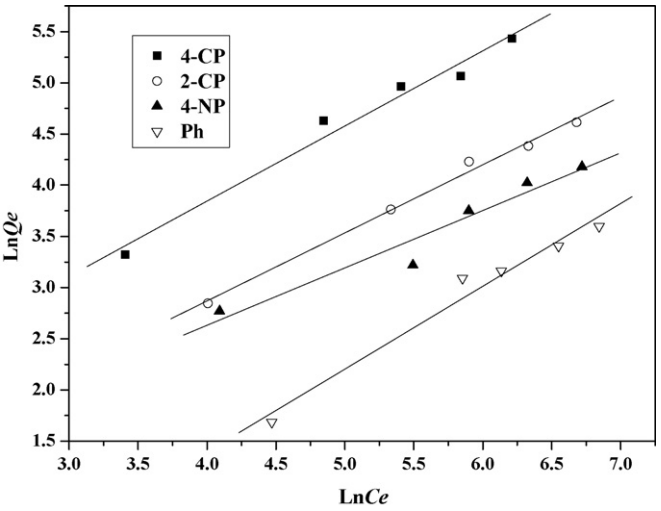

Fig. 14. Freundlich plot for different phenols adsorption onto TBP/Fe_3O_4@PSF microcapsules (contact time = 1 h; pH 6.0, 20 °C).

i.e. the adsorption of phenols on to TBP/Fe_3O_4@PSF microcapsules follows a multilayer adsorption process, and is not restricted to the formation of a monolayer.

3.4. The investigation of potential industrial application

3.4.1. Effect of adsorbent dose on the removal ratios of phenols

In order to investigate the effect of adsorbent dose on the removal ratios of phenols and to optimize the dose, a series of adsorption experiments was carried out. Varying amounts of TBP/Fe_3O_4@PSF microcapsules (5–30 g/L) were added to a 10 mL mixture of 4-CP (4.43 mg/L), 2-CP (4.66 mg/L), 4-NP (4.46 mg/L) and Ph (5.02 mg/L). The residual concentrations of phenols in the solu-

Table 2
The Langmuir and Freundlich equations, the related parameters and correlation coefficients for different phenols on TBP/Fe_3O_4@PSF microcapsules.

Compounds	Langmuir			Freundlich		
	$Q_{\max}$ (mg/g)	K_L (L/mg)	R^2	K_f (mg/g)(L/mg)$^{1/n}$	n	R^2
4-CP	370.4	0.0027	0.9061	2.482	1.362	0.9749
2-CP	158.7	0.0020	0.9695	1.232	1.503	0.9917
4-NP	102.0	0.0020	0.7824	1.475	1.783	0.9403
Ph	79.36	0.0009	0.8998	0.158	1.236	0.9739

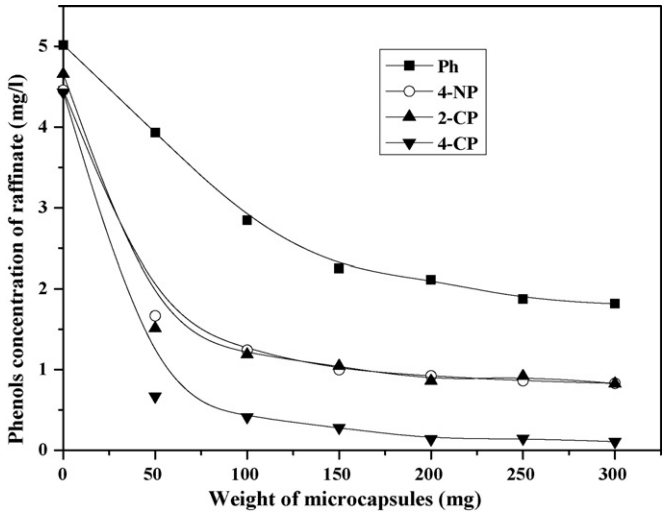

Fig. 15. Effect of weight of microcapsules on removal capability of phenols in aqueous solutions (10 mL of mixture containing 4-CP (4.43 mg/L), 2-CP (4.66 mg/L), 4-NP (4.46 mg/L) and Ph (5.02 mg/L); contact time = 1 h; pH 6.0, 20 °C).

Table 3
Removal ability (R) of regenerated TBP/Fe_3O_4@PSF microcapsules to phenols for six times.

Compounds	R_1 (%)	R_2 (%)	R_3 (%)	R_4 (%)	R_5 (%)	R_6 (%)
Ph	62.7	60.2	61.1	59.6	60.7	60.5
4-NP	80.6	71.9	71.5	70.9	69.9	70.1
2-CP	80.2	72.6	70.9	71.6	70.5	71.1
4-CP	96.7	81.5	80.5	79.9	80.2	80.9

tions after the adsorption were determined (Fig. 15). As can be seen from Fig. 15, the quantity of phenols removed increased with the increase in dosage of adsorbents up to certain levels, and then leveled off. The final concentration (4-CP (0.14 mg/L), 2-CP (0.92 mg/L), 4-NP (0.86 mg/L) and Ph (1.87 mg/L)) was within allowed limits when 250 mg of microcapsules were added. This indicates that the microcapsules do have a sufficient loading capacity for potential industrial applications.

3.4.2. Regeneration of microcapsules

To use the magnetic microcapsules on an industrial scale, it is necessary to make them easy to clean up. Therefore, regeneration of the loaded microcapsules and recovery of phenols in a concentrated form are key factors for improving the process economics. A successful desorption process must restore the sorbent close to its initial properties, for effective reuse. In this objective adsorption–regeneration cycles are realized, the removal capacity of phenols on to the microcapsules at every cycle was calculated using the following equation:

$$R(\%) = \frac{C_0 - C_e}{C_0} \times 100 \quad (6)$$

where C_0 and C_e are the initial and equilibrium concentrations of phenols solution (mg/L), respectively. As shown in Table 3, when up to five additional adsorption–regeneration cycles were performed, no decrease of adsorption capacity could be measured. This indicates that the microcapsules have great potential for industrial applications.

4. Conclusions

Magnetic microcapsules containing TBP have been prepared successfully and used for the adsorption of phenols from aqueous solution. The results show that it took about 30 min to reach extraction equilibrium, with most of the phenols being adsorbed within the first 5 min. The amount of the four phenols adsorbed under the same conditions was in the following order: 4-CP > 2-CP > 4-NP > Ph. Acid and neutral conditions were favorable for the adsorption. The adsorption process was well described with a Freundlich model. A two-stage kinetic behaviour has been confirmed, as the sorption rate followed a pseudo-second-order model. The results investigating potential industrial applications have demonstrated that the concentrations of the studied phenols decreased to the permitted level for effluent. After six repeated extraction and regeneration cycles, the microcapsules retained almost the same adsorption ability, indicating that the microcapsules have good stability. The experiments conducted in this work provided encouraging results for the application of these magnetic microcapsules to the adsorption of phenols from aqueous solutions in large-scale operations.

Acknowledgments

This work was supported by the National Natural Science Foundation of China Fund (no. 20775029), the Program for New Century Excellent Talents in University (NCET-07-0400), and the Central Teacher Plan of Lanzhou University.

References

[1] Y. Sun, J. Chen, A. Li, F. Liu, Q. Zhang, Adsorption of resorcinol and catechol from aqueous aqueous solution by aminated hypercrosslinked polymers, React. Funct. Polym. 64 (2005) 63–73.
[2] H. Polat, M. Molva, M. Polat, Capacity and mechanism of phenol adsorption on lignite, Int. J. Miner. Process. 79 (2006) 264–273.
[3] J. Wu, K. Rudy, J. Spark, Oxidation of aqueous phenol by ozone and peroxidase, Adv. Environ. Res. 4 (2000) 339–346.
[4] X. Hu, F.L.Y. Lam, L.M. Cheung, K.F. Chania, X.S. Zhao, G.Q. Lu, Removal of heavy metal ions fromwastewater by chemically modified plant wastes as adsorbents: a review, Catal. Today 68 (2001) 129–133.
[5] K. Abburi, Adsorption of phenol and p-chlorophenol from their single and bisolute aqueous solutions on Amberlite XAD-16 resin, J. Hazard. Mater. B 105 (2003) 143–156.
[6] C. Huang, Y.C. Huang, F.N. Tsai, Intraparticle diffusion-controlled kinetics of adsorption of phenol on ion exchange resins, Chem. Eng. Commun. 56 (1987) 77–85.
[7] F.A. Banat, B. Al-Bashir, S. Al-Ashes, O. Hayajnesh, Adsorption thermodynamics and kinetic investigation of aromatic amphoteric compounds onto different polymeric adsorbents, Environ. Pollut. 107 (2000) 391–398.
[8] S. Dutta, J.K. Basu, R.N. Ghar, Studies on adsorption of p-nitrophenol on charred saw-dust, Sep. Purif. Technol. 21 (2001) 227–235.
[9] M. Medir, A. Arriola, D. Mackay, F. Giralt, Phenol recovery from water effluents with mixed solvents, J. Chem. Eng. Data 30 (1985) 157–159.
[10] Z. Li, M. Wu, Z. Jiao, B. Bao, S. Lu, Extraction of phenol from wastewater by N-octonoylpyrrolidine, J. Hazard. Mater. B 114 (2004) 111–114.
[11] A. Dabrowski, P. Podkoscielny, Z. Hubicki, M. Barczak, Adsorption of phenolic compounds by activated carbon—a critical review, Chemosphere 58 (2005) 1049–1070.
[12] Z. Tong, Z. Qingxiang, H. Hui, L. Qin, Z. Yi, Q. Min, Kinetic study on the removal of toxic phenol and chlorophenol from waste water by horseradish peroxidase, Chemosphere 37 (1998) 1571–1577.
[13] M. Ahmaruzzaman, D.K. Sharma, Adsorption of phenols from wastewater, J. Colloid Interf. Sci. 287 (2005) 14–24.
[14] T. Ahsan, J.H. Wu, E.M. Arnett, Effects of citric acid washing on the thermodynamic interaction of some coals with acids, Fuel 73 (1994) 417–422.
[15] D. Batabyal, A. Sahu, S.K. Chaudhuri, Kinetics and mechanism of removal of 2,4-dimethyl phenol from aqueous solutions with coal fly ash, Sep. Technol. 5 (1995) 179–186.
[16] V.K. Gupta, I. Ali, V.K. Saini, Removal of chlorophenols from wastewater using red mud: an aluminum industry waste, Environ. Sci. Technol. 38 (2004) 4012–4018.
[17] V.K. Gupta, S. Sharma, I.S. Yadav, D. Mohan, Utilization of bagasse fly ash generated in sugar industry for the removal and recovery of phenol and p-nitrophenol from wastewater, J. Chem. Technol. Biotechnol. 71 (1998) 180–186.
[18] Y. Ku, K.C. Lee, Removal of phenols from aqueous solution by XAD-4 resin, J. Hazard. Mater. B 80 (2000) 59–68.
[19] S.H. Lin, R.S. Juang, Adsorption of phenol and it sderivatives from water using synthetic resins and low-cost natural adsorbents: a review, J. Environ. Manage. 90 (2009) 1336–1349.
[20] J. Fan, Y. Fan, Y. Pei, K. Wu, J. Wang, M. Fan, Solvent extraction of selected endocrine-disrupting phenols using ionic liquids, Sep. Purif. Technol. 61 (2008) 324–331.

[21] X.C. Gong, G.S. Luo, W.W. Yang, F.Y. Wu, Separation of organic acids by newly developed polysulfone microcapsules containing triotylamine, Sep. Purif. Technol. 48 (2006) 235–243.
[22] W.W. Yang, G.S. Luo, X.C. Gong, Extraction and separation of metal ions by a column packed with polystyrene microcapsules containing Aliquat 336, Sep. Purif. Technol. 43 (2005) 175–182.
[23] A.F. Ngomsik, A. Bee, J.M. Siaugue, D. Talbot, V. Cabuil, G. Cote, Co(II) removal by magnetic alginate beads containing Cyanex 272®, J. Hazard. Mater. 166 (2009) 1043–1049.
[24] A.F. Ngomsik, A. Bee, J.M. Siaugue, D. Talbot, V. Cabuil, G. Cote, Nickel adsorption by magnetic alginate microcapsules containing an extractant, Water Res. 40 (2006) 1848–1856.
[25] C.O. Illanes, N.A. Ochoa, J. Marchese, Kinetic sorption of Cr(VI) into solvent impregnated porous microspheres, Chem. Eng. J. 136 (2008) 92–98.
[26] W. Cao, B. Wang, Enrichment of phenolic compounds in water by tributyl phosphate extraction resin, Chin. J. Anal. Chem. 22 (1994) 609–611.
[27] X. Liu, Y. Guan, H. Liu, Z. Ma, Y. Yang, X. Wu, Preparation and characterization of magnetic polymer nanospheres with high protein binding capacity, J. Magn. Magn. Mater. 293 (2005) 111–118.
[28] G. Zhao, L. Zhou, Y. Li, X. Liu, Enhancement of phenol degradation using immobilized microorganisms and organic modified montmorillonite in a two-phase partitioning bioreactor, J. Hazard. Mater. 169 (2009) 402–410.
[29] S. Lu, J. Forcada, Preparation and characterization of magnetic polymeric composite particles by miniemulsion polymerization, J. Polym. Sci. Pol. Chem. 44 (2006) 4187–4203.
[30] H.S. Gao, J.M. Xing, X.C. Xiong, Immobilization of ionic liquid [BMIM][PF6] by spraying suspension dispersion method, Ind. Eng. Chem. Res. 47 (2008) 4414–4417.
[31] W.W. Yang, Y.C. Lu, Z.Y. Xiang, G.S. Luo, Monodispersed microcapsules enclosing ionic liquid of 1-butyl-3-methylimidazolium hexafluorophosphate, React. Funct. Polym. 67 (2007) 81–86.
[32] A. Breindl, B. Beck, T. Clark, Prediction of the n-octanol/water partition coefficient, logP, using a combination of semiempirical MO-calculations and a neural network, J. Mol. Model. 3 (1997) 142–155.
[33] P. Antonio, K. Ihac, M.E.V. Súarez-Iha, Kinetic modeling of adsorption of di-2-pyridylketone salicyloylhydrazone on silica gel, J. Colloid Interf. Sci. 307 (2007) 24–28.
[34] Y.S. Ho, G. McKay, The kinetics of sorption of divalentmetal ions onto sphagnum moss flat, Water Res. 34 (2000) 735–742.
[35] S.S. Gupta, K.G. Bhattacharyya, Removal of Cd(II) from aqueous solution by kaolinite, montmorillonite and their poly (oxo zirconium) and tetrabutylammonium derivatives, J. Hazard. Mater. B 128 (2006) 247–257.
[36] V.C. Srivastava, I.D. Mall, I.M. Mishra, Characterization of mesoporous rice husk ash (RHA) and adsorption kinetics of metal ions from aqueous solution onto RHA, J. Hazard. Mater. B 134 (2006) 257–267.
[37] W.J. Weber Jr., J.C. Morris, Kinetics of adsorption on carbon from solution, J. Sanit. Eng. Div. Proc. Am. Soc. Civil Eng. 89 (1963) 31–59.
[38] K. Kannan, M.M. Sundaram, Kinetics and mechanism of removal of methylene blue by adsorption on various carbons—a comparative study, Dyes Pigments 51 (2001) 25–40.
[39] M. Dogan, M. Alkan, A. Turkyılmaz, Y. Ozdemir, Kinetics and mechanism of removal of methylene blue by adsorption onto perlite, J. Hazard. Mater. B 109 (2004) 141–148.
[40] T.W. Weber, R.K. Chakkravorti, Pore and solid diffusion models for fixed-bed adsorbers, AIChE J. 20 (1974) 228.
[41] A.T. Mohd Din, B.H. Hameed, A.L. Ahmad, Batch adsorption of phenol onto physiochemical-activated coconut shell, J. Hazard. Mater. 161 (2009) 1522–1529.